

HUBBLE SPACE TELESCOPE FAR ULTRAVIOLET SPECTROSCOPY OF THE RECURRENT NOVA T PYXIDIS

PATRICK GODON¹, EDWARD M. SION¹, SUMNER STARRFIELD², MARIO LIVIO³, ROBERT E. WILLIAMS³,
CHARLES E. WOODWARD⁴, PAUL KUIN⁵, AND KIM L. PAGE⁶¹ Astronomy & Astrophysics, Villanova University, Villanova, PA 19085, USA; patrick.godon@villanova.edu, edward.sion@villanova.edu² School of Earth and Space Exploration, Arizona State University, Tempe, AZ 85287, USA; sumner.starrfield@asu.edu³ Space Telescope Science Institute, Baltimore, MD 21218, USA; mlivio@stsci.edu, wms@stsci.edu⁴ Minnesota Institute for Astrophysics, University of Minnesota, Minneapolis, MN 55455, USA; chelsea@astro.umn.edu⁵ Mullard Space Science Laboratory, University College London, Holmbury St. Mary, Dorking, Surrey RH5 6NT, UK; n.kuin@ucl.ac.uk⁶ Department of Physics & Astronomy, University of Leicester, Leicester, LE1 7RH, UK; klp5@leicester.ac.uk

Received 2014 January 13; accepted 2014 February 1; published 2014 March 19

ABSTRACT

With six recorded nova outbursts, the prototypical recurrent nova T Pyxidis (T Pyx) is the ideal cataclysmic variable system to assess the net change of the white dwarf mass within a nova cycle. Recent estimates of the mass ejected in the 2011 outburst ranged from a few $\sim 10^{-5} M_{\odot}$ to $3.3 \times 10^{-4} M_{\odot}$, and assuming a mass accretion rate of 10^{-8} – $10^{-7} M_{\odot} \text{ yr}^{-1}$ for 44 yr, it has been concluded that the white dwarf in T Pyx is actually losing mass. Using NLTE disk modeling spectra to fit our recently obtained *Hubble Space Telescope* COS and STIS spectra, we find a mass accretion rate of up to two orders of magnitude larger than previously estimated. Our larger mass accretion rate is due mainly to the newly derived distance of T Pyx (4.8 kpc, larger than the previous 3.5 kpc estimate), our derived reddening of $E(B - V) = 0.35$ (based on combined *IUE* and *GALEX* spectra), and NLTE disk modeling (compared to blackbody and raw flux estimates in earlier works). We find that for most values of the reddening ($0.25 \leq E(B - V) \leq 0.50$) and white dwarf mass ($0.70 M_{\odot} \leq M_{\text{wd}} \leq 1.35 M_{\odot}$) the accreted mass is larger than the ejected mass. Only for a low reddening (~ 0.25 and smaller) combined with a large white dwarf mass ($0.9 M_{\odot}$ and larger) is the ejected mass larger than the accreted one. However, the best results are obtained for a larger value of reddening.

Key words: accretion, accretion disks – binaries: close – novae, cataclysmic variables – stars: individual (T Pyxidis) – ultraviolet: stars – white dwarfs

Online-only material: color figures

1. INTRODUCTION

Cataclysmic variables (CVs) are binaries in which a white dwarf (WD; the primary) accretes hydrogen-rich material from a Roche-lobe filling secondary star. When sufficient matter is accreted, it undergoes a thermonuclear runaway (TNR), the classical nova eruption. The TNR ignition starts at the base of the accreted shell when the pressure and temperature are high enough for the CNO cycle burning of hydrogen (Paczynski 1965; Starrfield et al. 1972). CVs with recorded multiple nova outbursts are classified as recurrent novae (RNe). In RNe, a large mass WD and a high mass accretion rate are believed to lead to the short recurrence time between nova outbursts.

T Pyxidis (T Pyx), the prototypical RN, is known to have erupted (Webbink et al. 1987; Schaefer et al. 2013) in 1890, 1902, 1920, 1944, and 1967—roughly every ~ 20 yr. It erupted again in 2011 April (Waagan et al. 2011) after a lapse of 44 yr. The mass accreted between eruptions and the mass ejected during eruptions determine the net change in the WD mass. If the WD mass increases, then eventually it could reach the Chandrasekhar limit and explode as a Type Ia supernova (SN Ia; Whelan & Iben (1973); Iben & Tutukov (1984)). Due to its relatively frequent outbursts, T Pyx offers a promising possibility of assessing the WD mass change within a nova cycle. Recent works (Selvelli et al. 2008; Patterson et al. 2013; Nelson et al. 2012) have claimed that the WD in T Pyx is losing mass and will never become a SN Ia. In this Letter, we present a synthetic spectroscopic analysis of the first far ultraviolet (FUV; 900 Å–1700 Å) spectra of T Pyx obtained with *Hubble Space Telescope* (HST). Our objective is to estimate the rate of mass accretion following its 2011 July outburst and compare it with

estimates of the mass accretion rate in the quiescent interval preceding the 2011 July outburst.

2. SPECTRAL ANALYSIS

The most direct and accurate way to determine the mass accretion rate of a CV accreting at a high mass accretion rate is to carry out an analysis and modeling of its ultraviolet (UV; $\sim 900 \text{ \AA}$ – 3200 \AA) spectrum. This is because at a high mass accretion rate ($\sim 10^{-8} M_{\odot} \text{ yr}^{-1}$), an accretion disk around a WD emits more than 50% of its luminosity in the UV band (900 Å–3200 Å) and contributes much less to the optical. A significant fraction of the remaining energy is emitted in the extreme UV (EUV; $\lambda \sim 100 \text{ \AA}$ – 900 \AA), and that fraction increases with increasing mass accretion rate.

2.1. HST STIS + COS Spectroscopy of T Pyx

T Pyx was first observed in the UV ($\sim 1150 \text{ \AA}$ – 3200 \AA) with the *International Ultraviolet Explorer* (IUE). We co-added and combined 29 IUE spectra obtained with the Short Wavelength Prime (SWP; 1150 Å–2000 Å) camera and 11 IUE spectra obtained with the Long Wavelength Prime (LWP; 1850 Å–3200 Å) camera. These spectra, obtained between 1986 and 1996, exhibit the same continuum flux level. The IUE spectra show that the UV continuum of T Pyx remained nearly constant in slope and intensity, without any indication of long term trends, while the emission lines exhibit changes in both intensity and detectability as already mentioned by Gilmozzi & Selvelli (2007).

T Pyx was observed with the *Galaxy Evolution Explorer* (GALEX) at the end of 2005. The GALEX spectrum is composed

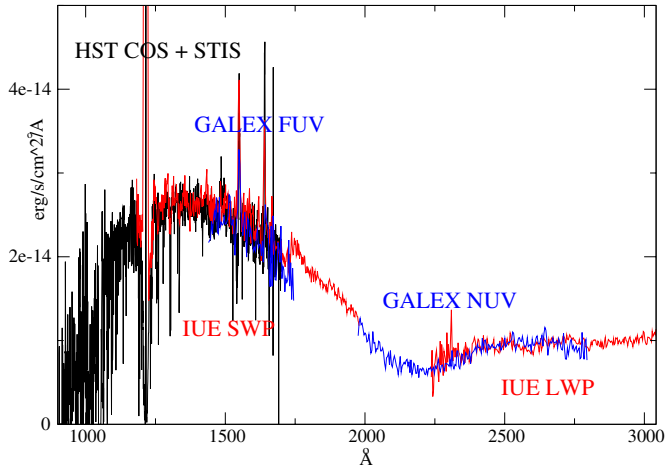


Figure 1. Existing UV spectra of T Pyx before and after its eruption. The archival *IUE* SWP and LWP spectra were obtained over a period of 10 yr and match both the *GALEX* and *HST* spectra. The noisy edges of the detectors have been removed for clarity. The UV (~ 1000 Å– 3000 Å) flux of T Pyx has remained fairly constant since it was first observed with *IUE*. This indicates that the mass accretion rate itself remained constant, and after its 2011 eruption it returned to its pre-outburst value.

(A color version of this figure is available in the online journal.)

of two spectra, one in the FUV band (1350 Å– 1800 Å) and one in the near UV (NUV) band (1800 Å– 3000 Å). In spite of detector edge problems, the *GALEX* and *IUE* spectra match remarkably well in those regions away from the edges, in agreement with the suggestion (Gilmozzi & Selvelli 2007) that the UV continuum remains constant over the years. This is an indication that *the mass accretion rate itself is constant*, since the UV emission comes mainly from the accretion disk. Consequently, the steady decline of the optical magnitude of T Pyx, observed since 1890, does not indicate a decrease in the mass accretion rate.

FUV (1150 Å– 2250 Å) spectra of T Pyx were obtained with the *HST*/Space Telescope Imaging Spectrograph (STIS) during the eruption and the decline to quiescence (Shore et al. 2013). We further followed T Pyx into quiescence, obtaining *HST*/STIS spectra (~ 1150 Å– 1700 Å) together with *HST*/Cosmic Origins Spectrograph (COS) spectra (~ 900 Å– 1200 Å) in 2012 March, 2012 December, and 2013 July. While the 2012 March spectrum still exhibits strong emission lines and a flux larger than the pre-outburst flux level, the 2012 December and 2013 July spectra have weak emission lines and have reached the pre-outburst flux level of the *IUE* and *GALEX* spectra. Except for small differences in emission lines, the 2012 December and 2013 July *HST* spectra are identical, and show that T Pyx has now returned precisely to its pre-outburst value (i.e., *IUE* flux level). This indicates that the mass accretion rate has returned to its pre-outburst value.

Since the 2012 December and 2013 July *HST* spectra are almost identical, we co-added them to improve the signal-to-noise ratio (S/N) in preparation for the spectral model fit. In Figure 1 we show the quiescent co-added *IUE*, *GALEX*, and co-added *HST* spectra after removal of the noisy detector edges. The spectra, though acquired with different telescopes and instruments, match accurately. The minimum near 2175 Å is due to interstellar extinction. Since the *GALEX* spectrum is the most reliable in that wavelength region, we combine it with the *IUE* co-added spectrum to determine $E(B - V)$. We then deredden the combined spectrum for different values of $E(B - V)$. The $E(B - V)$ value for which the 2175 Å feature

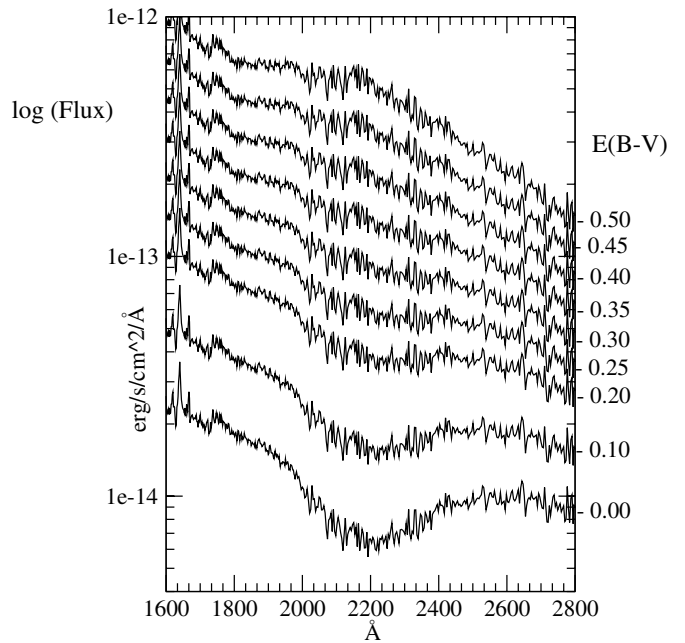


Figure 2. Merged *GALEX*–*IUE* spectrum (see Figure 1) dereddened for different values of $E(B - V)$ as indicated on the right. The 2175 Å feature associated with the reddening is clearly seen in absorption for low values of $E(B - V)$, and it appears as extra flux (“emission-” like) for large values of $E(B - V)$. We deduce that the reddening toward T Pyx must be $E(B - V) = 0.35$, the value for which the 2175 Å region vanishes (i.e., it becomes rather flat and featureless on the log graph).

disappears, $E(B - V) = 0.35$ (see Figure 2), is taken as the $E(B - V)$ value toward T Pyx, in agreement with Bruch et al. (1981). We use this value to deredden the *IUE*, *GALEX*, and *HST* spectra, but we also consider the effects of different reddening values on our results.

We combined the *HST* (STIS+COS), *IUE*, and *GALEX* spectra, excluding the noisy portions, and obtained a spectrum from ~ 900 Å to ~ 3200 Å. While we modeled the entire spectrum, we never expected the model to fit in the NUV range (~ 2000 Å– 3000 Å) because we only modeled the hottest component of the system, the accretion disk, which mainly contributes to the FUV (~ 900 Å– 1700 Å) and extreme UV (~ 100 Å– 900 Å). The shorter wavelengths of the spectrum covered by COS are crucial in determining the mass accretion rate as this is where the spectrum is expected to peak if the accretion rate is large.

2.2. Modeling

The disk is the standard disk model (Shakura & Sunyaev 1973; Pringle 1981), and for a given mass accretion rate and a given WD mass, it is divided into N rings with temperature T_i , ($i = 1, 2, \dots, N$) located at $r = r_i$, ($i = 1, 2, \dots, N$), where $T_i = T_{\text{eff}}(r_i)$, and $T_{\text{eff}}(r)$ is the radial temperature profile of the standard disk model (e.g., Pringle (1981)). Each ring is modeled using the stellar atmosphere code TLUSTY. Then a synthetic spectrum is computed with the code SYNSPEC for each ring, and the spectra are finally combined together with DISKSYN, taking into account Keplerian broadening, inclination, and limb darkening (Hubeny 1988; Hubeny & Lanz 1995; Wade & Hubeny 1998). For rings with $T > 30,000$ K TLUSTY and SYNSPEC are run with basic NLTE options.

To emphasize the importance of modeling the disk in the UV, we use our disk modeling to check what fraction of the disk

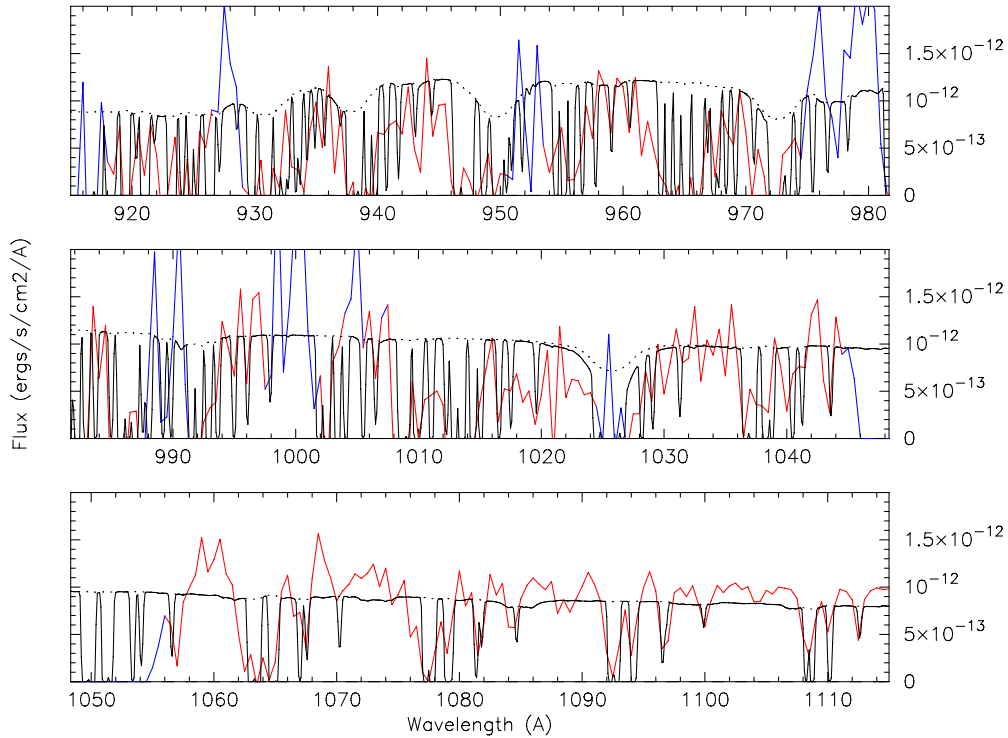


Figure 3. *HST* COS spectrum (in red) of T Pyx fitted with a disk model (solid black line) including an interstellar medium (ISM) absorption curtain (the dotted line indicates the disk model without ISM absorption). The COS data are rather noisy. The regions marked in blue are either due to noise, airglow, or emission lines, and are not modeled. The fitting is carried out between the solid black line and the solid red line. The gap between 1045 Å and 1055 Å is a detector gap. The spectrum has been dereddened assuming $E(B - V) = 0.35$. At a distance of 4.8 kpc, the flux in the COS spectrum is accounted for with a large mass accretion rate. In this model we have $M_{\text{wd}} = 0.7 M_{\odot}$, $i = 20^{\circ}$, $\dot{M} = 2.4 \times 10^{-6} M_{\odot} \text{ yr}^{-1}$. For an accretion period of 44 yr, this gives a total accreted mass of $\sim 10^{-4} M_{\odot}$.

(A color version of this figure is available in the online journal.)

luminosity is emitted in the UV band ($900 \text{ \AA} < \lambda_{\text{UV}} < 3200 \text{ \AA}$). For a canonical WD mass of $0.8 M_{\odot}$, at a mass accretion rate of $10^{-9.5} M_{\odot} \text{ yr}^{-1}$ the disk emits 58% of its luminosity in the UV band (λ_{UV}), and most of the remaining luminosity ($\sim 40\%$) is emitted at longer wavelengths. As the mass accretion rate increases, so does the temperature in the disk. At $\dot{M} = 10^{-9}$ the disk emits 66% of its luminosity in the UV, about 30% at longer wavelengths, and only a few percent in the EUV ($\lambda < 900 \text{ \AA}$). As the mass accretion rate keeps increasing, the disk starts emitting more flux in the EUV and less flux in the UV and optical, as the Planckian peak shifts to shorter and shorter wavelengths. At $\dot{M} = 10^{-8} M_{\odot} \text{ yr}^{-1}$, the disk emits $\sim 50\%$ in the UV with about 25% emitted at shorter wavelengths and 25% emitted at longer wavelengths. The amount emitted in the visual band is just a fraction of the 25% and is always much less than the amount emitted in the UV band. This justifies the modeling of accretion disk in the UV band. The main source of the optical luminosity is not from the disk, but most likely arises from the contribution from the hot spot, the secondary, and possibly from some of the nebular material.

From theoretical predictions, to reproduce an outburst every 20 yr or so, the WD mass in T Pyx is expected to be very large (almost near-Chandrasekhar). On the other hand, the derived mass ratio $q = 0.2$ in the system together with an *anticipated* secondary mass of $M_2 = 0.14 M_{\odot}$ imply a WD mass of only $M_{\text{wd}} = 0.7 M_{\odot}$ (Uthas et al. 2010). However, the secondary has never been spectroscopically detected to verify the assumption $M_2 = 0.14 M_{\odot}$. Consequently, due to the uncertainty in the WD mass, we generated disk models for an accreting WD with a near-Chandrasekhar mass of $1.35 M_{\odot}$ as expected from the observed short recurrence time of T Pyx (Starrfield et al. 1985;

Webbink et al. 1987; Schaefer et al. 2010), and for a lower mass WD, $0.70 M_{\odot}$, as inferred by Uthas et al. (2010). The latter low mass, if confirmed, raises serious problems for the theory of recurrent shell flashes. We varied the mass accretion rate, \dot{M} , from $\sim 10^{-9} M_{\odot} \text{ yr}^{-1}$ to $\sim 10^{-6} M_{\odot} \text{ yr}^{-1}$. The inclination (i) of the system is low with a lower limit of about $i = 10^{\circ}$ (Uthas et al. 2010) and an upper limit of $i = 30^{\circ}$ (Webbink et al. 1987). Since we model only the continuum, the effect of the inclination on the results is very small, as long as the inclination is low. For a given WD mass (and therefore radius), the fitting of the observed spectrum with a theoretical accretion disk spectrum is carried out by scaling the theoretical flux to the distance of 4.8 kpc, which has been recently derived using the light echo technique (Sokoloski et al. 2013).

3. RESULTS

We first fit the dereddened spectrum assuming $E(B - V) = 0.35$. For the $M_{\text{wd}} = 1.35 M_{\odot}$ case, we found a mass accretion rate of $\dot{M} = 1.6 \times 10^{-6} M_{\odot} \text{ yr}^{-1}$ for $i = 10^{\circ}$ and $\dot{M} = 1.9 \times 10^{-6} M_{\odot} \text{ yr}^{-1}$ for $i = 30^{\circ}$. The total mass accreted over 44 yr (since the previous explosion) is $7.0 \times 10^{-5} M_{\odot}$ and $8.4 \times 10^{-5} M_{\odot}$, for $i = 10^{\circ}$ and $i = 30^{\circ}$, respectively. For the $M_{\text{wd}} = 0.70 M_{\odot}$ case, the mass accretion rate needed to fit the spectrum increases to $\dot{M} = 2.2 \times 10^{-6} M_{\odot} \text{ yr}^{-1}$ and $2.7 \times 10^{-6} M_{\odot} \text{ yr}^{-1}$, for $i = 10^{\circ}$ and $i = 30^{\circ}$, respectively; the total accreted mass becomes $9.7 \times 10^{-5} M_{\odot}$ and $1.2 \times 10^{-4} M_{\odot}$. A synthetic accretion disk model spectral fit to the *HST*/COS spectrum is presented in Figure 3 for $M_{\text{wd}} = 0.7 M_{\odot}$ and an inclination of $i = 20^{\circ}$. The exact same spectral fit to the *HST*/STIS spectrum and combined *GALEX-IUE* spectrum is

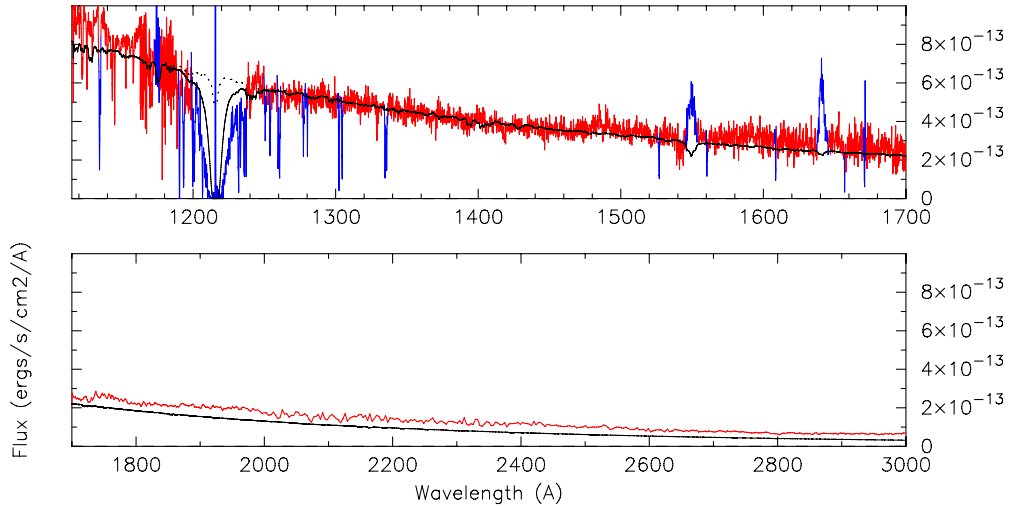


Figure 4. Same model fit shown in Figure 1 is shown here in the longer wavelengths, covering mainly the STIS and *IUE* range. The Ly α region ($\sim 1200 \text{ \AA} - 1240 \text{ \AA}$) is affected by the ISM and is therefore not modeled. The sharp emission and absorption lines are also not included in the modeling. From $\sim 1600 \text{ \AA}$ and longward into the *IUE* LWP range, the observed spectrum has extra flux possibly due to a colder component in the system.

(A color version of this figure is available in the online journal.)

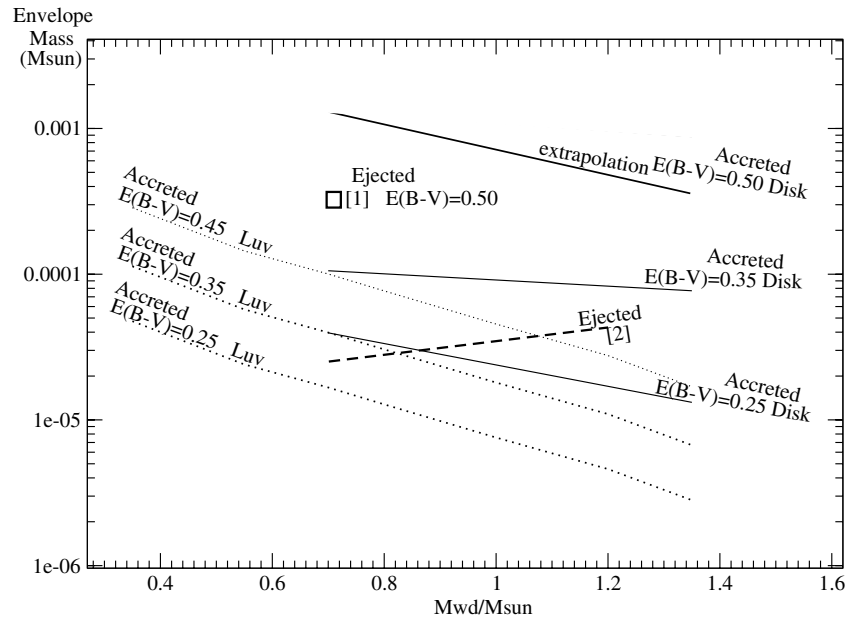


Figure 5. Mass of the accreted envelope and ejected envelope are shown as a function of the WD mass for different values of the reddening. Our disk model results are drawn with a solid line (“Disk”). The lower limit of the accreted envelope inferred from the UV flux is shown (dotted line; “Luv”). In comparison we show the ejected envelope [1] as estimated by Nelson et al. (2012; square symbol), as well as [2] computed in Patterson et al. (2013; dashed line). The ejected estimate [1] was computed assuming $E(B - V) = 0.5$ and $M_{\text{wd}} = 0.7 M_{\odot}$ and is to be compared with our result for the same value of $E(B - V)$ and M_{wd} . The accreted envelope is always larger than the ejected envelope, except for a value of $E(B - V) = 0.25$ combined with a WD mass $\sim 0.9 M_{\odot}$ and larger. However, the best results were obtained for a larger value of the reddening $E(B - V) > 0.30$, as the $E(B - V) = 0.25$ value led to either a very bad fit or a distance of only ~ 1 kpc. The accreted envelope for the $E(B - V) = 0.50$ case (marked “extrapolation”) has been carried out by linearly extrapolating our accretion disk models, and is an underestimate (this is more pronounced for the $1.35 M_{\odot}$ WD mass case).

presented in Figure 4. The synthetic spectrum is deficient in flux in the longer wavelength range, $\lambda > 1600 \text{ \AA}$, indicating the possible contribution of a colder component ($T < 10,000 \text{ K}$).

Even though we derived a reddening of 0.35, which is consistent with the originally derived $E(B - V)$ value from the *IUE* data in Bruch et al. (1981), we nevertheless checked the effect of the reddening on the results (since different methods and reddening curves for evaluating $E(B - V)$ lead to different results (e.g., Shore et al. 2013; see also Gilmozzi & Selvelli 2007)).

Based on *IUE* data alone, Gilmozzi & Selvelli (2007) derived a reddening value of $E(B - V) = 0.20 - 0.25$. We therefore checked our fitting results for the value of $E(B - V) = 0.25$, and we found that to fit the distance of 4.8 kpc one needs a mass accretion rate of $9 \times 10^{-7} M_{\odot} \text{ yr}^{-1}$ ($i = 20^{\circ}$). However, this synthetic spectrum does not fit the slope of the observed spectrum; the observed spectrum is too red. To fit the slope of the spectrum one needs a much lower mass accretion rate, namely $M = 10^{-8} M_{\odot} \text{ yr}^{-1}$, but the resultant flux level produced is lower which requires a distance to T Pyx of only 1250 pc.

Similar results are obtained for this reddening when assuming a $1.35 M_{\odot}$ WD mass.

Next, for a larger reddening value of $E(B - V) = 0.5$ (Shore et al. 2013), the observed spectrum is too *blue*, and our models are limited by the constraint that TLUSTY does not handle mass accretion rates greater than $5 \times 10^{-6} M_{\odot} \text{ yr}^{-1}$ for a $0.7 M_{\odot}$ WD mass and $1 \times 10^{-6} M_{\odot} \text{ yr}^{-1}$ for a $1.35 M_{\odot}$ WD mass. We extrapolated our results linearly by matching flux level; namely, we assume that the flux level is a linear function of the mass accretion rate and we ignore Wien’s displacement. Since the Planckian peaks move toward shorter wavelengths as \dot{M} increases, this extrapolation underestimates \dot{M} , and this effect is more pronounced as \dot{M} increases. Using this technique, we found that the mass accretion rate needed to fit the observed spectrum assuming $E(B - V) = 0.5$ for a $M_{\text{wd}} = 0.7 M_{\odot}$ (as in Shore et al. 2013) is $\dot{M} = 3 \times 10^{-5} M_{\odot} \text{ yr}^{-1}$, implying a total accreted mass of $1.32 \times 10^{-3} M_{\odot}$. For the $1.35 M_{\odot}$ WD mass case, this linear extrapolation gives a mass accretion rate of $8 \times 10^{-6} M_{\odot} \text{ yr}^{-1}$ and a total accreted mass of $3.5 \times 10^{-4} M_{\odot}$.

4. CONCLUSIONS

Our results are recapitulated in Figure 5, where we draw (solid lines) the mass accreted over 44 yr as computed from our model fittings, for three different values of the reddening. We also draw (dotted line) the lower limit for the accreted mass derived from integrating the UV flux over the wavelengths 900 Å to 3200 Å

$$\Delta M_{\text{min}} = 44 \times \dot{M}_{\text{min}} = 44 \times \int F_{\lambda} d\lambda.$$

Since the disk at a high mass accretion rate emits only a fraction of its energy in the UV (and a much smaller fraction is emitted in the optical), the integrated UV flux is clearly a lower limit for the mass accretion rate. We draw this lower limit for three different values of the reddening as well. For comparison we draw the ejecta mass as derived by radio observations by Nelson et al. (2012; denoted with a square, #1), who assumed $M_{\text{wd}} = 0.7 M_{\odot}$ and $E(B - V) = 0.50$. This ejecta mass is to be compared with our accreted mass derived from our disk modeling, assuming $E(B - V) = 0.50$. Our results show that the accreted envelope (for the particular values of the parameters) is about four times larger than the mass ejected as estimated by Nelson et al. (2012). On the graph, we also show the mass of the ejected envelope as estimated by Patterson et al. (2013), assuming that energy and momentum are conserved (dashed line, #2). We see that the disk model fittings imply that more mass is accreted than ejected, except when assuming a reddening of $E(B - V) = 0.25$ in combination with a WD mass $M_{\text{wd}} > 0.9 M_{\odot}$. However, for this value of the reddening, the disk model (for all WD masses considered) did not fit the observed spectrum, indicating that the reddening might indeed be larger (i.e., 0.35).

We note that the $\sim 10\%$ error in the distance 4.8 ± 0.5 kpc translates into an error of the order of 20% in the mass accretion rate, which does not change our results significantly. We also emphasize that the difference between our results and previously derived mass accretion rates is due mainly to the now larger distance estimates (4.8 kpc versus 3.5 kpc) as well as a larger reddening (0.35 versus 0.25).

In this Letter, we: (1) determine the long-time baseline accretion rate in T Pyx, using for the first time realistic disk

models, and (2) demonstrate that the accretion rate in T Pyx has returned to exactly its pre-outburst UV spectral energy distribution. This accretion rate, $\sim 10^{-6} M_{\odot} \text{ yr}^{-1}$ (and higher for increasing values of the reddening), is much higher than previously estimated.

It is possible that T Pyx sustains such a high mass accretion rate because of irradiation of the secondary star. The irradiation of the donor star by the extremely hot WD and inner disk will not only “puff up” the donor’s radius but may also drive wind off the secondary (Knigge et al. 2000). Since the orbital period and binary separation of T Pyx are smaller than all other known RNe, the effects of irradiation may be more pronounced.

Several different authors reported that quasi-static evolutionary sequences of accreting WDs expand into red giant structures at accretion rates exceeding $10^{-7} M_{\odot} \text{ yr}^{-1}$ (Paczynski & Zytkov 1978; Sion et al. 1979; Iben 1982) but other evolutionary accreting WD sequences followed hydrodynamically through multiple nova outbursts (e.g., Prialnik & Kovetz 1995; Yaron et al. 2005; Starrfield et al. 2012; Idan et al. 2013) reveal thermonuclear shell flashes at these high rates.

This research is supported by HST grants GO-12799.01A and GO-12890.01A, both to Villanova University. Support for the analysis of the *IUE* and *GALEX* archival data was provided by the National Aeronautics and Space Administration (NASA) under grant No. NNX13AF11G issued through the Office of Astrophysics Data Analysis Program (ADP) to Villanova University. P.G. thanks William P. Blair for his kind hospitality at the Henry A. Rowland Department of Physics and Astronomy at the Johns Hopkins University, Baltimore, MD. We also thank Steve Shore for his comments on the manuscript.

REFERENCES

- Bruch, A., Duerbeck, H. W., & Seitter, W. C. 1981, *MitAG*, **52**, 34
 Gilmozzi, R., & Selvelli, P. 2007, *A&A*, **461**, 593
 Hubeny, I. 1988, *CoPhC*, **52**, 103
 Hubeny, I., & Lanz, T. 1995, *ApJ*, **439**, 875
 Iben, I. 1982, *ApJ*, **259**, 244
 Iben, I., & Tutukov, A. V. 1984, *ApJS*, **54**, 335
 Idan, I., Shaviv, N. J., & Shaviv, G. 2013, *MNRAS*, **433**, 2884
 Knigge, C., King, A. R., & Patterson, J. 2000, *A&A*, **364**, L79
 Nelson, T., et al. 2012, *ApJ*, submitted (arXiv:1211.3112)
 Paczyński, B. 1965, *AcA*, **15**, 197
 Paczyński, B., & Zytkov, A. N. 1978, *ApJ*, **222**, 604
 Patterson, J., et al. 2013, in *ASP Conf. Ser., Stella Novae: Past and Future Decades*, ed. P. A. Woudt & V. A. R. M. Ribeiro, in press
 Prialnik, D., & Kovetz, A. 1995, *ApJ*, **445**, 789
 Pringle, J. E. 1981, *ARA&A*, **19**, 137
 Schaefer, B. E., Landolt, A. U., Linnolt, M., et al. 2013, *ApJ*, **773**, 55
 Schaefer, B. E., Pagnotta, A., & Shara, M. 2010, *ApJ*, **708**, 381
 Selvelli, P., Cassatella, A., Gilmozzi, R., & González-Riestra, R. 2008, *A&A*, **492**, 787
 Shakura, N. I., & Sunyaev, R. A. 1973, *A&A*, **24**, 337
 Shore, S. N., Schwarz, G. J., De Gennaro Aquino, I., et al. 2013, *A&A*, **549**, 140
 Sion, E. M., Acierno, M. J., & Tomczyk, S. 1979, *ApJ*, **230**, 832
 Sokolowski, J., Crotts, A. P. S., Lawrence, S., & Uthas, H. 2013, *ApJL*, **770**, L33
 Starrfield, S., Sparks, W. M., & Truran, J. W. 1985, *ApJ*, **291**, 136
 Starrfield, S., Timmes, F. X., Iliadis, C., et al. 2012, *BaltA*, **21**, 76
 Starrfield, S., Truran, J. W., Sparks, W. M., & Kutter, G. S. 1972, *ApJ*, **176**, 169
 Uthas, H., Knigge, C., & Steeghs, D. 2010, *MNRAS*, **409**, 237
 Waagan, E., Linnolt, M., Bolzoni, S., et al. 2011, *CBET*, **2700**, 1
 Wade, R. A., & Hubeny, I. 1998, *ApJ*, **509**, 350
 Webbink, R. F., Livio, M., Truran, J. W., & Orio, M. 1987, *ApJ*, **314**, 653
 Whelan, J., & Iben, I. 1973, *ApJ*, **186**, 1007
 Yaron, O., Prialnik, D., Shara, M. M., & Kovetz, A. 2005, *ApJ*, **623**, 398